

# ELICITATION OF PARABOLIC BEAM AND CONFINEMENT WELL USING PATTERN RECOGNITION OVER UV-Vis SPECTRA OF GOLD NANO SPHERES

M.F. YILMAZ<sup>1</sup>, M. OZDEMIR<sup>1</sup>, Y. DANISMAN<sup>2</sup>, B.KARLIK<sup>3</sup>, O.O. AGA<sup>4</sup>, C.T.YAVUZ<sup>5</sup>

<sup>1</sup>Basic Sciences, College of Engineering, University of Dammam, KSA

<sup>2</sup>Department of Mathematics, University of Oklahoma, Norman, OK, USA

<sup>3</sup>Independent Researcher, Montreal, QC, CANADA

<sup>4</sup>Environmental Engineering, College of Engineering, University of Dammam, KSA

<sup>5</sup>Graduate School of EEWS, Korea Advanced Institute of Science and Technology, 291 Daehak-ro, Yuseong-gu, Daejeon 305-701, Republic of Korea

## ABSTRACT

In this study, Mie scattering calculated spectra of gold nanospheres (GNS) with different diameters are used as a database for the purpose of principal component (PCA) and linear discriminant analysis (LDA) of pattern recognition. PCA and LDA extract the hidden structures of the database by the corresponding vectors or coefficients. 3D representation of coefficients obtained by PCA of spectral database results in a non-diffractive (airy) beam of surface plasmon polaritons (SPP) in the shape of parabola. The eigen spectra obtained as a result of PCA exhibit the dipole surface plasmon resonances, and Fano-like resonances. 3D representation of LDA coefficients of database acts as a quantum well in a way of confining of the electrons. Eigen spectra out of LDA illustrate the oscillation wave patterns of ions and electrons. Extracted PCA coefficients of database are arranged for the training of Artificial Neural Network for the estimation of the diameters of GNS. In the end, experimental spectra of diameters of GNS are tested and compared with the ANN outputs and DLS measurements. PCA based ANN estimates the GNS diameters with the high accuracy. Moreover, our results show that application of PCA and LDA with corresponding spectra can be made use of as an alternative way of diagnosing light-nanoparticles interactions.

## I. INTRODUCTION

The arrangement of metal nanoparticles in an order of chain or array provides surface plasmon polaritons (SPPs), which are the bosonic (quasiparticles) coupled modes of an incident electromagnetic wave and free electrons (plasmon) of surface. SPPs can manipulate the radiation and perform as the micro-optical devices[1,2]. Furthermore, airy plasmon polaritons are the non diffractive version of SPPs, which can propagate in undistorted manner for several diffraction lengths along the metal surface [3]. For these advantages, nanoparticles have potential applications in nanophotonics, nanoscale imaging and sensing and biomedicine[4].

The measurement of the diameters of nanoparticles is important as the size of the diameter is known to be related to both the optical performance and the risk of nanoparticles on human health. There is a number of techniques to measure the size of a nano particle, and none of these techniques is superior to the other. Some of these techniques are Scanning electron microscopy, Atomic Force Microscopy, Photon correlation spectroscopy and so on. There are also computational techniques

that can estimate diameter size such as Mie scattering theory. Besides, principal component and linear discriminant analysis (PCA and LDA) and artificial neural network (ANN) for pattern recognition techniques are used to estimate diameters of nano particles [5 and 6].

PCA and LDA are the two of the most common statistical techniques that are used in order to reduce the dimension of a given raw data in pattern recognition problems. The PCA function is an unsupervised procedure used for the analysis of the inherent multivariate structure of the data, and the main aim of the PCA is to retain the subspace of a dataset that has the greatest variance. PCA uses rotation as the linear transformation in a way that most of the data variability remains in a space of few dimension, and it ignores the remaining dimensions containing little variability. PCA basically transforms the data to a new coordinate system. LDA as a pattern recognition technique has a quite similar approach to that of PCA. The main difference stems from the fact that LDA considers class labels while projecting the feature space onto a smaller space. The idea of LDA is to determine the vector that best separates classes while trying to keep variance maximum. So, LDA is a supervised techniques that take different classes in a data set into account whereas PCA discards class differences by treating all data set as single featured and finds the directions that maximize variance in a data set. Although it looks like LDA outperforms PCA in multi-class settings where class labels are known, it might not be the case especially if the sizes of the classes in the data set are relatively small. Besides, LDA performs well only if the classes have equal co-variance. PCA is good at keeping dimensions of highest variance, but it can disregard discriminant dimensions where LDA is needed. It is easy to find examples where LDA outperforms PCA and vice versa [7,8,9, 10 and 11].

The ANN algorithms also have been of high potential interest and used over the last couple of decades in many realtime applications and various areas such as remote sensing, computer vision, pattern recognition and medical diagnosis. The ANN can easily identify and extract the patterns by setting correlation between some set of given inputs and outputs through a training process. Especially, their adaptative nature allows solving complex and non-linear problems. Another advantages of ANN is the fact that it can establish strong correlation between the parameters without any knowledge of them. Therefore, it enables to handle uncertainties, data with noise and relationships which are nonlinear and hard to determine [6,12,13,14 and 15]. Besides, ANNs have been applied, to study X-ray spectroscopy to predict plasma electron temprature and densities, to UV- Vis and infrared spectroscopy for investigating forensics [16 and 17]. Latterly, they have been used to estimate the diameters of nanoparticles [6].

In this work, we have employed Mie scattering calculated spectra of GNS as our database. This database is first analysed by PCA and LDA methods, and then the physical intepretations of PCA and LDA of UV-vis spectra of gold are examined. Then, the extracted PCA coefficients are used for the training purpose for ANN to estimate the diameters of GNS. In the end, experimental spectra of gold spheres with diameters 5,7,10,15,20 and 30 nm are tested for the estimation of diameters [18].

Corresponding author: fthyilmaz53@gmail.com

## II. Experimental Section

Hydrogen tetrachloroaurate (III) trihydrate ( $\text{HAuCl}_4 \cdot 3\text{H}_2\text{O}$ , gold salt), trisodium citrate (reducing agent), and sodium chloride were obtained from Aldrich and used as received. Gold nanoparticles (AuNPs) with the sizes of 5, 7, 10, 15, 20 and 30 nm (see Fig.1) were purchased from Nanocomposix, Inc. Distilled water was used to prepare the aqueous solutions of AuNPs. Au nanoparticles were synthesized through the well-established reduction methods of Turkevich, Frens and Murphy [19, 20 and 21]. In the preparation of 5 nm AuNPs, a 10 mL aqueous solution containing 0.25 mM  $\text{HAuCl}_4$  and 0.25 mM trisodium citrate was first prepared. Ice-cooled 0.3 mL of 0.1 M sodium borohydride was added to this solution while stirring. The color change in the solution was an indication of the particle formation.

For the synthesis of 7 nm or larger AuNPs, aqueous solutions of 0.254 mM  $\text{HAuCl}_4$  and 38.8 mM trisodium citrate were first prepared. In a typical synthesis, 50 mL  $\text{HAuCl}_4$  solution was heated to boiling. After 5 min., 0.4-2.0 mL trisodium citrate solution was added to this mixture at once and the mixture was stirred for approximately 15 min. The colour of the reaction mixture was turned from yellow to colourless and then ruby red colour depending on the AuNPs sizes. After cooling to RT, the samples were centrifuged and washed several times with DI water to obtain 5, 7, 10, 15, and 30 nm citrate-coated AuNPs.

Dynamic light scattering (DLS, Malvern Zetasizer Nano ZS) technique was used to determine the average hydrodynamic diameters of gold nanoparticles. Nano ZS detects the scattered light at an angle of  $173^\circ$ , known as backscatter detection, by using He-Ne laser (4 mW) operated at 633 nm. Aqueous 10 mM NaCl solutions were used for all DLS measurements.

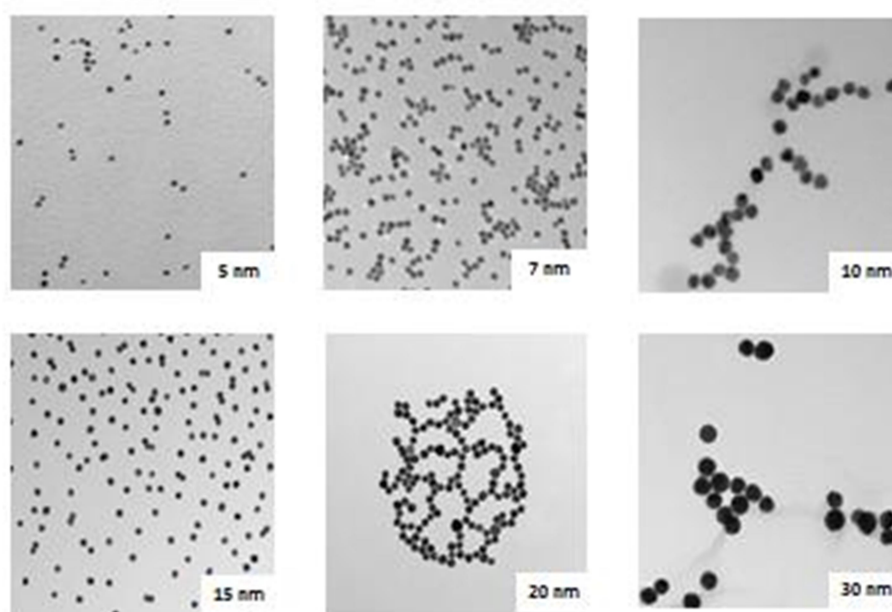


Fig.1.TEM images of gold nanoparticles

### III. MIE SCATTERING

The Mie theory is known to be the theory that is used for the absorption and scattering of an electromagnetic plane wave through a homogeneous sphere. Although Mie theory is based on idealized initial conditions, it is widely used for the radiation problems in a light scattering media. This theory mainly calculates the coefficients for absorption, scattering and extinction. One can find a number of programs that can perform Mie solutions. The main advantage of the Mie solution stems from the fact that it suggests solutions for the cases where the diameter of scattering particle is comparable to the wavelength of the light. For the cases where the diameter of scattering particle is much larger or smaller than the wavelength of the light, there are already simple methods that can be used in order to describe the behaviour of the corresponding system. Since our case is the former one, we employed Mie theory calculated spectra to create our database [18]. Our database contains 25 spectra of gold spheres without polymer shell with the diameters 2, 4, 6, 10, ..., 50 nm. In Fig.2 experimental spectra of 5, 7, 10, 15 and 30 nm and their Mie calculated spectra are illustrated. From these spectra, we generated 101 eigenvalues with 101 corresponding eigenvectors of which we took the ones that correspond to the first and the second greatest eigenvalues for our PCA analysis.

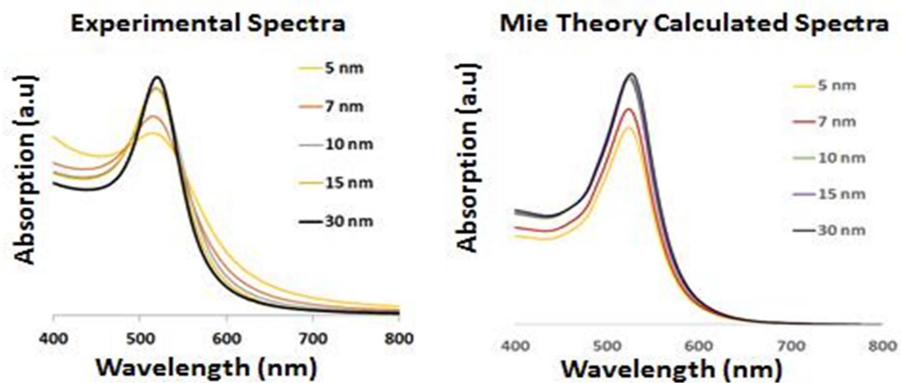


Fig2. Experimental spectra and Mie calculated spectra

### IV. Principal Component Analysis

In this section, we give an overview of PCA by following the work of Jolliffe and Herta et al. in [22 and 23] and more details can be found in [24]. The main purpose of PCA is to find a subspace spanned by the vectors with largest variances. This is an optimization problem, which reduces the dimension of a data set while retaining the variance. This goes through by converting the data set of possibly correlated variables into linearly uncorrelated variables called Principal Components (PC). These PCs determine the similarities and differences of the data, and they are the eigenvectors of the covariance matrix which consists of covariances of all different dimensions. Hence, every element of the original data can be written as a linear combination of PCs. To reduce the dimension, only the eigenvectors which correspond to the largest (dominant) eigenvalues of the covariance matrix are considered. The original data is projected into the space spanned by these PCs which are orthonormal. In this way, some information is lost due to not considering the eigenvectors correspond to the small eigenvalues, but this information has less significance.

For  $i=1,2,\dots,M$  let  $\Gamma_i$  be the vectors in a data set of size  $N \times 1$ . The mean of  $\Gamma_i$ 's is

$$\mu = \frac{1}{M} \sum_{i=1}^M \Gamma_i \quad (1)$$

Now subtract the mean  $\mu$  from each of  $\Gamma_i$  and define

$$\Phi_i = \Gamma_i - \mu \quad (2)$$

The covariance matrix  $\mathbf{C}$  is

$$\mathbf{C} = \frac{1}{M} \sum_{i=1}^M \Phi_i \Phi_i^t = \frac{1}{M} \mathbf{A} \mathbf{A}^t \quad (3)$$

Where, superscript  $t$  means transpose and  $\mathbf{A} = [\Phi_1, \Phi_2, \dots, \Phi_M]$ .  $\mathbf{C}$  is an  $N \times N$  symmetric matrix. It is diagonosable and has  $N$  nonnegative eigenvalues and eigenvectors. The eigenvector corresponding to the largest eigenvalue is called the first principal component ( $|PC1\rangle$ ) and the second and third largest ones are called the second ( $|PC2\rangle$ ) and the third principal component ( $|PC3\rangle$ ). If a vector  $|v\rangle$  is projected into the space spanned by  $|PC1\rangle$ ,  $|PC2\rangle$  and  $|PC3\rangle$  then we have

$$\text{Proj}_{\langle |PC1\rangle, |PC2\rangle, |PC3\rangle} |v\rangle = w_1 |PC1\rangle + w_2 |PC2\rangle + w_3 |PC3\rangle \quad (4)$$

The coefficients  $w_1$ ,  $w_2$  and  $w_3$  are called the weights of  $|PC1\rangle$ ,  $|PC2\rangle$  and  $|PC3\rangle$  in  $|v\rangle$  and they are equal to following equations respectively;

$$w_1 = |v\rangle \cdot (|PC1\rangle)^t \quad (5)$$

$$w_2 = |v\rangle \cdot (|PC2\rangle)^t, \quad (6)$$

$$w_3 = |v\rangle \cdot (|PC3\rangle)^t, \quad (7)$$

where  $\cdot$  is the dot product in Euclidean space ( $\mathbb{R}^N$ ). Since  $|PC1\rangle$ ,  $|PC2\rangle$  and  $|PC3\rangle$  are the most dominant two eigenvectors, the vector  $v - (w_1 |PC1\rangle + w_2 |PC2\rangle + w_3 |PC3\rangle)$  has less significance and it can be ignored. Therefore, it is enough to work on the three dimensional space spanned by  $|PC1\rangle$ ,  $|PC2\rangle$  and  $|PC3\rangle$ .

Fig.3a illustrates the mean absorbance and vector representation of the spectra.  $|PC1\rangle$  vector spectrum represents the dipole surface Plasmon resonance, and  $|PC2\rangle$  vector spectrum which is perpendicular to the  $|PC1\rangle$  vector represents asymmetric line shape of Fano like resonance. Fano resonance which is resulted by the interference of the scattering amplitudes of continuous (bright mode) and discrete states (dark mode) and provides a field enhancement [25 and 26].

In Fig.3a 3D representation of PCA coefficients of GNS is shown. The parabolic bend in this plot describes the path that non-diffractive (airy) beam of surface Plasmon polariton wave follows during

its travel. This behavior is observed in the array structures of nanoparticles. Since our database is generated by the spectra of different diameters of gold nanospheres in an ascending order, such an array behavior is expected [27].

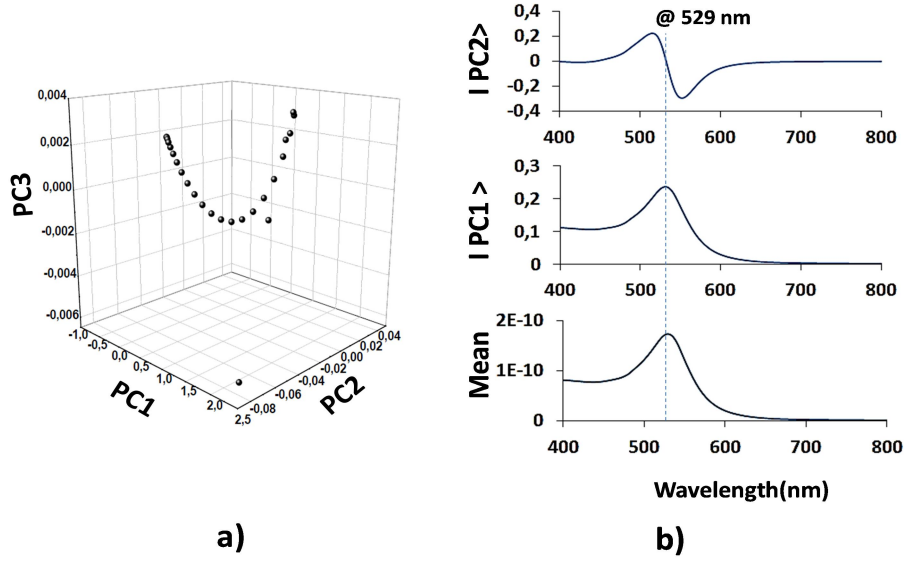


Fig.3 a)  $|PC1\rangle$ ,  $|PC2\rangle$  and  $|PC3\rangle$  coefficients in 3D, b) mean,  $|PC1\rangle$  and  $|PC2\rangle$  spectra

## V. Linear Discriminant Analysis

Linear Discriminant Analysis (LDA) is another dimension reduction technique to identify the hidden structures of a large data [28]. LDA is applied to a data which consists of different classes of similar elements and used to find vectors, like principal components of PCA, to discriminate the classes while respecting the similarities among the class members. The main idea in LDA is to project a data onto a smaller subspace as in PCA but with a good class separability. In contrary, PCA deals with the entire data and does not consider the different classes. Therefore, LDA is applied to a data when different classes must be considered.

Let  $K$  be the number of classes, which consists of  $M$  elements of size  $N \times 1$ , in a data. Let  $\Gamma_i^j$  be the  $i$ th element of the class  $j$  for  $i=1,2,\dots,M$  and  $j=1,2,\dots,K$  where  $\Gamma_i^j$  is a  $N \times 1$  vector.

Within-class scatter matrix  $S_w$  is

$$S_w = \sum_{j=1}^K \sum_{i=1}^M (\Gamma_i^j - \mu_j) (\Gamma_i^j - \mu_j)^t, \quad (8)$$

where  $\mu_j$  is the mean of the class  $j$  and superscript  $t$  means the transpose. Between class scatter matrix  $S_b$  is

$$S_b = \sum_{j=1}^K (\mu_j - \mu) (\mu_j - \mu)^t, \quad (9)$$

where  $\mu$  is the mean of all classes. In LDA, the eigenvectors of  $(S_w)^{-1} S_b$  provides the vectors that will be used basis for the new vector space. The eigenvectors correspond to the largest two eigenvalues

are called the first dominant eigenvector ( $|LD1\rangle$ ), second ( $|LD2\rangle$ ) and third dominant eigenvector ( $|LD3\rangle$ ). As in the PCA case, projection of a vector  $|v\rangle$  into the space spanned by  $|LD1\rangle$  and  $|LD2\rangle$  is

$$\text{Proj}_{\langle |LD1\rangle, |LD2\rangle, |LD3\rangle} |v\rangle = w_1^l |LD1\rangle + w_2^l |LD2\rangle + w_3^l |LD3\rangle \quad (10)$$

The coefficients  $w_1^l$ ,  $w_2^l$  and  $w_3^l$  are called the weights of  $|LD1\rangle$ ,  $|LD2\rangle$  and  $|LD3\rangle$  in  $|v\rangle$  and they are equal to

$$w_1^l = |v\rangle \cdot (|LD1\rangle)^t, \quad w_2^l = |v\rangle \cdot (|LD2\rangle)^t \quad \text{and} \quad w_3^l = |v\rangle \cdot (|LD3\rangle)^t, \quad (11)$$

In Fig.4a, LDA coefficients in 3D exhibits electron confinement well structure. Such confinements are expected as the size of the particle decreases to nanoscale comparable to the electron's wavelength. The electrons in these structures behave like a particle in potential well. Confined standing waves are the time independent solutions of the Schrodinger equations in the potential well which are formed by concurring of two anti-propagating surface plasmon waves respectively [29 and 30]. Fig. 4b shows the LDA vector spectra which illustrate the oscillating wave pattern of ions( $|LD1\rangle$ ) and electrons( $|LD2\rangle$ ) respectively [31 and 32].

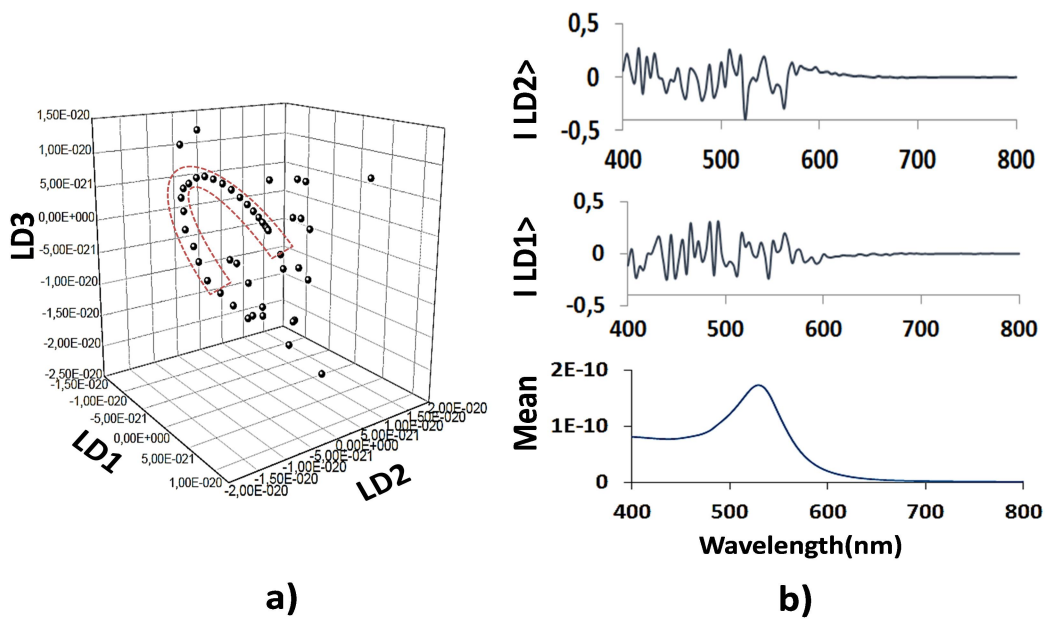


Fig.4 a) LD1, LD2 and LD3 coefficients and b)  $|LD1\rangle$  and  $|LD2\rangle$  spectra.

## VI. ARTIFICIAL NEURAL NETWORKS

One of the most effective features of artificial neural networks is to adapt their behavior to the changing characteristics of the used modeled system. As a parallel processing distributed system artificial neural networks (ANNs) are depend on learn through a training set of data using a learning algorithm[33]. The processing units in feed forward and back-propagation neural networks are arranged in mostly multi layered perceptron (MLP) architectures which has back-propagation (BP) algorithm using various different activation functions. Most commonly used non-linear activation

functions are the sigmoid and the hyperbolic tangent functions [34]. As seen in Fig.5, each layer of MLP is fully connected to the previous layer, and has no other connection. The MLP consists of 3 or more layers including one input, one output and one or more hidden layers. Multiple hidden layers of non-linearly activating nodes make a deep neural network. In this study we used 4 layered MLP architecture which consists of 1 number of nodes of input layer, 5 number of nodes for both hidden layer.

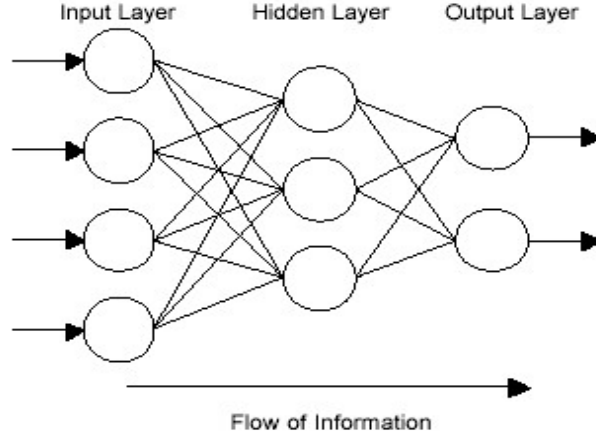


Fig. 5. Illustration of general MLP architecture

The BP with generalized delta learning rule with an iterative gradient algorithm is implemented to minimize the mean square error (MSE) between the actual output of a multilayered feed-forward neural network and a target output. MSE is also used to measure how well ANN works. The purpose is to make MSE small enough by choosing appropriate  $w_{ji}$  and  $\theta_j$ . MLP neural network train and learn from a set of given data in order to determine the values of the weights. Learning takes place through constantly changing the weights and comparing the amount of errors to find the best one that approximate the expected result. To predict the correct output by obtaining minimum error ( $E$ ) for each pattern ( $p$ ) by subtracting the overall output ( $o$ ) from the target ( $t$ ). To realize this purpose, a pattern  $p \in P$  is chosen successively and randomly, and then  $w_{ji}$  and  $o_j$  are changed by [35]. Following equations show the basic ones of classic error back-propagation algorithm.

$$o_j = f(net_j) = f(x) \text{ if } net_j = \sum_j w_{ji} o_i + \theta_j \quad (12)$$

$$E_p = \frac{1}{2} \sum_{j \in \text{output}} (t_{pj} - o_{pj})^2 \quad (13)$$

$$\begin{aligned} \delta_{pj} &= (t_{pj} - o_{pj}) \\ \Delta_p w_{ji} &= -\varepsilon \left( \frac{\partial E_p}{\partial w_{ji}} \right) \\ \Delta_p \theta_j &= -\varepsilon \left( \frac{\partial E_p}{\partial \theta_j} \right) \end{aligned} \quad (14)$$



In the operation element, if, as transfer (threshold) function, it is used "sigmoid" one;

$$o_{pj} = \frac{1}{\sum_i 1 + e^{-w_{ji}o_{pi} + \theta_j}} \quad (15)$$

$$(\text{net}p_j) = \sum_i w_{ji}o_{pi} + \theta_j$$

it is derived the equation 15 and done necessary shortening;

$$\frac{\partial o_{pj}}{\partial \text{net}p_j} = o_{pj}(1 - o_{pj}) \quad (16)$$

If this is replaced in equation 14, for output element;

$$\delta_{pj} = (t_{pj} - o_{pj})o_{pj}(1 - o_{pj}) \quad (17)$$

If this gradient descent algorithm is extended for any number of hidden layers, it is defined as

$$\delta_{pj} = o_{pj}(1 - o_{pj}) \sum_k \delta_{pk} w_{kj} \quad (18)$$

If it is added momentum term to the general equation set to speed up the computation of the algorithm, in the most general condition, it is given output and hidden layer equations as follows:

$$\begin{aligned} \Delta_p w_{ji}(t+1) &= \varepsilon \delta_{pj} o_{pi} + \alpha \Delta_p w_{ji}(t) \\ \Delta_p \theta_j(t+1) &= \varepsilon \delta_{pj} + \alpha \Delta_p \theta_j(t) \end{aligned} \quad (19)$$

where, t represents the number of iteration,  $\alpha$  is momentum coefficient, and  $\varepsilon$  is learning rate[36]. In this study, the learning rate and momentum coefficients are chosen to be 0.1 and 0.95 respectively.

Figure 6 shows there is a nonlinear relation between the extracted PCA and LDA coefficients and the corresponding diameters. PCA coefficients which are obtained from the spectra produced from Mie scattering theory are used for the training process as inputs, and the outputs are the diameters of the nanoparticles. In this setting, it should be pointed out that PCA method provides an advantage for the use of ANNs as it enables to reduce the dimensions of inputs. Since LDA of spectra of GNSs reveals electron dynamics with extreme non-linearity (see Fig. 6b), LDA based ANN was not studied in this work.

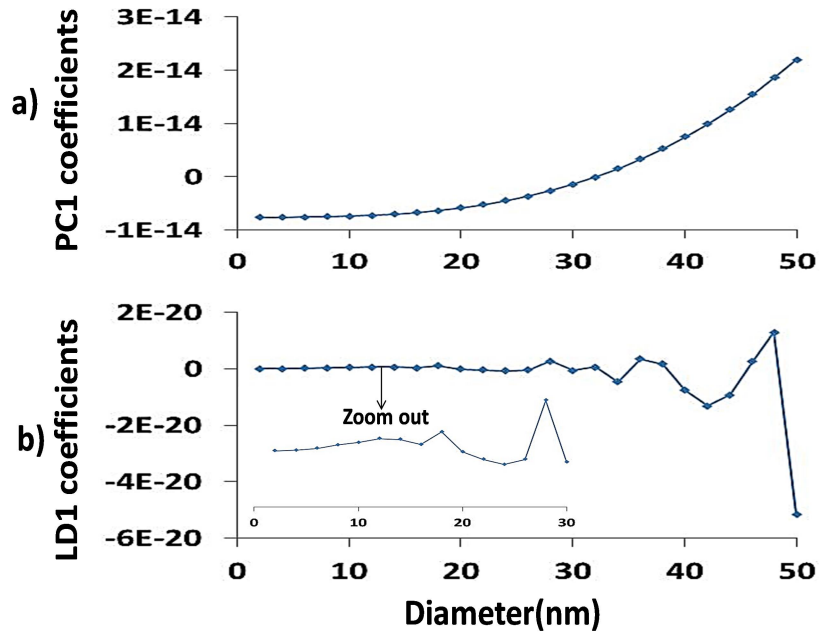


Fig.6 Plot of a) Coefficients of  $|PC1\rangle$  and b)  $|LD1\rangle$  versus GNS diameters

In Table 1, Dynamic Light Scattering(DLS) measurements of gold spheres and ANN estimations of diameters are presented. ANN estimations show that average testing error was found as 2,0966 for 6 different diameters. In other words, the recognition accuracy was 97,903%.

GNSP(nm)	DLS Diameters (nm)	PCA Based ANN Diameters (nm)	Percentage Errors with PCA based ANN (%)
5	5±0.6	4.5055	9.89
7	7.5±0.8	7.0458	0.65
10	11.6±1	10.1730	1.7
15	15.4±1.5	15.0101	0.06
20	20.5±2.1	20.0205	0.09
30	31±3	30.0687	0.19

Table 1. Values of measured and estimated diameters with error

## VII. CONCLUSION

Our results show that PCA and LDA can be used as an alternative method to diagnose light-GNS interactions. PCA of spectral database reveals the propagation and polarization dynamics. LDA of spectra reveals the quantum well confinement structure and nonlinear electron dynamics. After calculation of PCA coefficients, a nonlinear relation between them and the particle diameters is observed. It was thanks to PCA coefficients that we are able to reduce the dimension of input data for the training of ANN, and thereby simplifying the inputs and outputs of ANN modeling. ANN estimation of experimental data shows that ANN is a powerful tool for estimating the diameters with high accuracy. Because, the recognition accuracy after testing has been obtained as 97,903% for 6 different diameters. ANN model is a useful method in terms of saving time and cost by predicting the results of the proposed model. In conclusion, it turns out that Pattern recognition based ANN is a powerful method for estimating the diameters of nanoparticles which is of significance due to reasons mentioned above.

## ACKNOWLEDGEMENTS

Special thanks to Nanocomposix Inc. for providing TEM images and measurements of nanoparticles and MIE scattering calculator.

## LIST OF REFERENCES

1. Petryayeva, E., & Krull, U. J. (2011). Localized surface plasmon resonance: nanostructures, bioassays and biosensing—a review. *Analytica chimica acta*, 706(1), 8-24.
2. Evlyukhin, A. B., Bozhevolnyi, S. I., Stepanov, A. L., Kiyan, R., Reinhardt, C., Passinger, S., & Chichkov, B. N. (2007). Focusing and directing of surface plasmon polaritons by curved chains of nanoparticles. *Optics express*, 15(25), 16667-16680.
3. Salandrino, A., & Christodoulides, D. N. (2010). Airy plasmon: a nondiffracting surface wave. *Optics letters*, 35(12), 2082-2084.
4. Shopa, M., Kolwas, K., Derkachova, A., & Derkachov, G. (2010). Dipole and quadrupole surface plasmon resonance contributions in formation of near-field images of a gold nanosphere. *Opto-Electronics Review*, 18(4), 421-428.
5. Martínez, J. C., Chequer, N. A., González, J. L., & Cordova, T. (2012). Alternative methodology for gold nanoparticles diameter characterization using PCA technique and UV-Vis spectrophotometry. *Nanoscience and Nanotechnology*, 2(6), 184-189.
6. Shabanzadeh, P., Senu, N., Shameli, K., Ismail, F., Zamanian, A., & Mohaghehtabar, M. (2015). Prediction of silver nanoparticles' diameter in montmorillonite/chitosan bionanocomposites by using artificial neural networks. *Research on Chemical Intermediates*, 41(5), 3275-3287.

7. L.I. Smith, A Tutorial on Principal Components Analysis, vol. 51, Cornell University, USA, 2002, p. 52.
  
8. Cho, H., & Moon, S. (2009, August). Comparison of PCA and LDA based face recognition algorithms under illumination variations. In *ICCAS-SICE, 2009* (pp. 4025-4030). IEEE.
  
9. Yilmaz, M. F., Danisman, Y., Larour, J., & Aranchuk, L. (2015). Principal component analysis of electron beams generated in K-shell aluminum X-pinch plasma produced by a compact LC-generator. *High Energy Density Physics, 15*, 43-48.
  
10. Wold, K. Esbensen, P. Geladi, Principal component analysis, *Chemom. Intell Lab. Syst.* 2 (1) (1987) 37-52.
  
11. M. Zamalloa, L.J. Rodriguez-Fuentes, M. Penagarikano, G. Bordel, J.P. Uribe, Comparing genetic algorithms to principal component analysis and linear discriminant analysis in reducing feature dimensionality for speaker recognition, in: *Proceedings of the 10th Annual Conference on Genetic and Evolutionary Computation, ACM, 2008*, pp. 1153-1154.
  
12. I.Y. Khan, P.H. Zope, S.R. Suralkar, Importance of Artificial Neural Network in Medical Diagnosis disease like acute nephritis disease and heart disease, *Int. J. Eng. Sci. Innovat. Technol.* 2 (2013) 210-217.
  
13. Y. Guo, K. De Jong, F. Liu, X. Wang, C. Li, A comparison of artificial neural networks and support vector machines on land cover classification, in: *Proc. of the 6th Int. Symp. on Intelligence Computation and Applications (ISICA 2012), Communication in Computer and Information Science* , vol. 316, 2012, pp. 531e539.
  
14. A. Eleyan, H. Demirel, PCA an LDA based face recognition using feed forward neural network classifier, multimedia content representation, classification and security, *Lect. Notes Comput. Sci.* 4105 (2006) 199e206.
  
15. Asadnia, M., Khorasani, A. M., & Warkiani, M. E. (2017). An Accurate PSO-GA Based Neural Network to Model Growth of Carbon Nanotubes. *Journal of Nanomaterials, 2017*.
  
16. Yilmaz, M. F., Eleyan, A., Aranchuk, L. E., & Larour, J. (2014). Spectroscopic analysis of X-pinch plasma produced on the compact LC-generator of Ecole Polytechnique using artificial neural networks. *High Energy Density Physics, 12*, 1-4.
  
17. Larour, J., Aranchuk, L. E., Danisman, Y., Eleyan, A., & Yilmaz, M. F. (2016). Modeling of the L-shell copper X-pinch plasma produced by the compact generator of Ecole polytechnique using pattern recognition. *Physics of Plasmas, 23*(3), 033115.
  
18. Steven J. Oldenburg, *Light scattering from gold nanoshells*. Diss. Rice University, 2000.
  
19. Frens, G. (1973). Controlled nucleation for the regulation of the particle size in monodisperse gold suspensions. *Nature physical science, 241*, 20-22.

20. Turkevich, J., Stevenson, P. C., & Hillier, J. (1951). A study of the nucleation and growth processes in the synthesis of colloidal gold. *Discussions of the Faraday Society*, 11, 55-75.
21. Jana, N. R., Gearheart, L., & Murphy, C. J. (2001). Seeding growth for size control of 5– 40 nm diameter gold nanoparticles. *Langmuir*, 17(22), 6782-6786.
22. Jolliffe, I.T., *Principal Component Analysis*, Springer Series in Statistics, New York, 2002, 489 p.
23. Hastie, T., Tibshirani, R., Friedman, J. The elements of statistical learning. Data mining, Inference, and prediction. 2<sup>nd</sup> edition. Springer, 2009.
24. Danisman, Y., Yilmaz, M. F., Ozkaya, A., & Comlekçiler, I. T. (2014). A comparison of eigenvalue methods for principal component analysis. *Appl. Comput. Math*, 13(3).
25. Zhu, Z., Bai, B., You, O., Li, Q., & Fan, S. (2015). Fano resonance boosted cascaded optical field enhancement in a plasmonic nanoparticle-in-cavity nanoantenna array and its SERS application. *Light: Science & Applications*, 4(6), e296.
26. Kong, X., Qiu, L., & Xiao, G. (2017). *Fano Resonance in High-Permittivity Objects. In Resonance. InTech*.
27. Li, L., Li, T., Wang, S. M., Zhang, C., & Zhu, S. N. (2011). Plasmonic Airy beam generated by in-plane diffraction. *Physical review letters*, 107(12), 126804.
28. A. Tharwat, T. Gaber, A. Ibrahim and A. E. Hassanien, Linear discriminant analysis: A detailed tutorial. *AI Communications*, 30(2), 169-190, (2017).
29. Crommie, M. F., Lutz, C. P., & Eigler, D. M. (1993). Confinement of electrons to quantum corrals on a metal surface. *Science*, 262(5131), 218-220.
30. Fang, Y., & Tian, X. (2014). Resonant surface plasmons of a metal nanosphere can be considered in the way of propagating surface plasmons. arXiv preprint arXiv:1412.2664.
31. Yilmaz, M. F., Tanrıseven, M. E., Obonyo, E., Ergul, M., Danisman, Y., & Ozdemir, M. (2018). Linear Discriminant Analysis As An Alternative Method To Investigate The Interaction Of A 1064 Nm Cw Laser Light With A Cold Inductively-Coupled Plasma. arXiv preprint arXiv:1802.05729.
32. Ross, A. E., & McKenzie, D. R. (2016). Predator-prey dynamics stabilised by nonlinearity explain oscillations in dust-forming plasmas. *Scientific reports*, 6, 24040.
33. Kizilaslan, R., and Karlik, B. (2009). Combination Neural Networks Forecasters for Monthly Natural Gas Consumption Prediction. *Neural Network World*, 19 (2), 191-199.
34. Karlik, B. and Olgac, A.V. (2011) Performance Analysis of Various Activation Functions in Generalized MLP Architectures of Neural Networks. *International Journal of Artificial Intelligence and Expert Systems*. 1(4) 111-122.
35. Karlik, B. (2003). A Neural Network Image Recognition for Control of Manufacturing Plant. *Mathematical & Computational Applications*. 8 (2), 181-189.

36. Gulez, K., Mutoh, N., Harashima, F., Pastaci, H., Karlik, B. (2000) Fault Diagnosis and Performance Increment of an Induction Motor with Simultaneous Neural Network Approximations. CCSP'2000 (International Conference on Communications, Control & Signal Processing in the Next Millennium), 331-335, July 25-28, 2000, Bangalore, India.